JACS Au
AN OPEN ACCESS JOURNAL OF THE AMERICAN CHEMICAL SOCIETY



pubs.acs.org/jacsau
Letter

# Concerted Hydrosilylation Catalysis by Silica-Immobilized Cyclic Carbonates and Surface Silanols

Shingo Hasegawa, Keisuke Nakamura, Kosuke Soga, Kei Usui, Yuichi Manaka, and Ken Motokura*

Cite This: JACS Au 2023, 3, 2692−2697
Read Online

ACCESS | Metrics & More | Article Recommendations | Supporting Information

**ABSTRACT:** Developing a method for creating a novel catalysis of organic molecules is essential because of the growing interest in organocatalysis. In this study, we found that cyclic carbonates immobilized on a nonporous or mesoporous silica support showed catalytic activity for hydrosilylation, which was not observed for the free cyclic carbonates, silica supports, or their physical mixture. Analysis of the effects of linker lengths and pore sizes on the catalytic activity and carbonate C═O stretching frequency revealed that the proximity of carbonates and surface silanols was crucial for synergistic hydrosilylation catalysis. A carbonate and silanol concertedly activated the silane and aldehyde for efficient hydride transfer. Density functional theory calculations on a model reaction system demonstrated that both the carbonate and silanol contributed to the stabilization of the transition state of hydride transfer, which resulted in a reasonable barrier height of 16.8 kcal mol$^{-1}$. Furthermore, $SiO_2$/carbonate(C4) enabled the hydrosilylation of an aldehyde with an amino group without catalyst poisoning, owing to the weak acidity of surface silanols, in sharp contrast to previously developed acid catalysts. This study demonstrates that immobilization on a solid support can convert inactive organic molecules into active and heterogeneous organocatalysts.

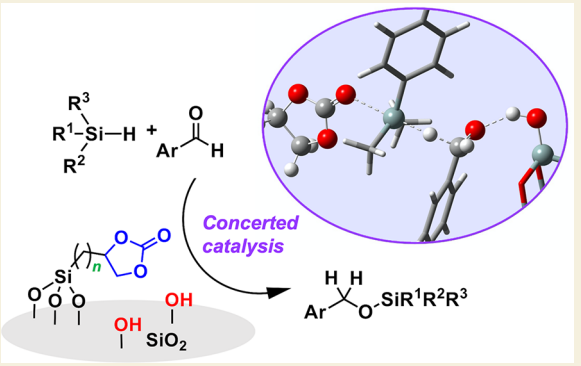


**KEYWORDS:** *concerted catalysis, surface immobilization, heterogeneous organocatalyst, cyclic carbonate, hydrosilylation*

Since the pioneering works on organocatalysts around 2000,[1−4] this class of catalysts has attracted great interest, particularly as an essential component for the environmentally benign and efficient synthesis of fine chemicals.[5−13] Thus, the creation of novel organocatalysts is important, and one promising method is the immobilization of organic molecules on a solid support. It has been demonstrated that catalysis of organic functional groups and metal complexes was improved via surface immobilization.[14−26] Silica supports reportedly enhance the catalytic activity of immobilized functional groups, owing to the weak acidic nature of surface silanols. Kubota and Sugi found that catalytic activity of secondary amines for aldol reaction is increased by a mesoporous silica additive and that the promotional effect is more prominent for silica-immobilized amines than for the physical mixture.[14] Katz and co-workers deconvoluted polarity and acidity environmental effects in supported catalysts involving tethered amine-on-silica sites, using Knoevenagel, Michael, and nitroaldol reactions, and correlated results with salicylaldehyde bonding as a probe of polarity and acidity.[15,16] Jones and co-workers conducted detailed studies on the effect of pore size and linker length on the catalytic activity of mesoporous-silica-supported amines for aldol and nitroaldol reactions.[17−21] Nevertheless, all of these supported catalysts contain amines, which are well-known for their base catalytic properties. The creation of novel surface-enhanced catalysis of an organic molecule that has never been used as a catalyst is an attractive research target to open a new avenue for organocatalysis.

Cyclic carbonates are an important group of compounds[27−29] that are easily synthesized from $CO_2$ and extensively used as aprotic polar solvents and electrolytes for batteries. The highly polarized structures of cyclic carbonates indicate their potential as Lewis base organocatalysts, although their catalytic application has not been reported. Thus, the cyclic carbonate structure was chosen as the active site of the novel immobilized organocatalysts.

In this study, we demonstrated that the immobilization of cyclic carbonates on silica with specific linker lengths led to the emergence of hydrosilylation catalysis. Effects of structural parameters on the catalytic activity and the carbonate C═O stretching frequency were systematically investigated. We propose that carbonate and silanol concertedly activate the

Received: June 13, 2023
Revised: September 10, 2023
Accepted: September 11, 2023
Published: September 15, 2023

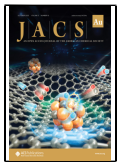





https://doi.org/10.1021/jacsau.3c00306
JACS Au 2023, 3, 2692−2697

silane and aldehyde, respectively, for efficient hydride transfer, which was supported by theoretical calculations. The immobilized catalyst was applicable to a substrate with an amino group because of the weak acidity of silanols, which is in sharp contrast to that of previously reported acid catalysts. Thus, we have demonstrated that surface immobilization can trigger the emergence of novel organocatalysis.

Physicochemical properties of support materials used in this study were reported elsewhere.[30] Nonporous-silica-supported cyclic carbonates having different methylene linker lengths, $SiO_2$/carbonate(C*n*), were prepared by a silane coupling reaction using 78 $\mu$mol of carbonate(C*n*) and 75 mg of $SiO_2$, as shown in Scheme 1. Mesoporous-silica-supported catalysts,

**Scheme 1. Preparation of Catalysts**

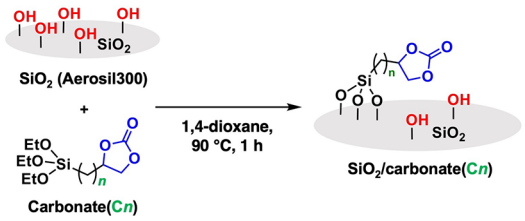


MS(*x*)/carbonate(C*n*) (*x*: pore size in Å), were obtained by a similar procedure. The equivalence of silanol to carbonate before immobilization was 5.9−7.4, according to $^{29}$Si dd/MAS NMR.[30] The carbonate(C*n*) precursors were synthesized from epoxyolefins in two steps (Scheme S1): (1) epoxyolefins were converted into epoxides with a terminal Si(OEt)$_3$ group by hydrosilylation with triethoxysilane and a Rh or Pt catalyst and (2) the cycloaddition of $CO_2$ to the epoxide catalyzed by silica-supported tetrabutylammonium iodide afforded carbonate-(C*n*).[31] The results of elemental analysis in Table S1 indicated the successful immobilization of the carbonates on the support with the carbon content increasing with increasing linker length. Fourier-transform infrared (FT-IR) spectroscopy further confirmed the presence of carbonates on silica (Figure 1a), and absorption bands corresponding to the C═O and C−H stretching modes of the carbonate moiety were observed for the prepared catalysts. Solid-state $^{13}$C cross-polarization/magic angle spinning nuclear magnetic resonance (CP/MAS NMR) spectroscopy indicated retention of the cyclic carbonate structure (Figure 1b). $^{29}$Si CP/MAS NMR analysis using $SiO_2$/carbonate(C4) as a representative catalyst revealed that

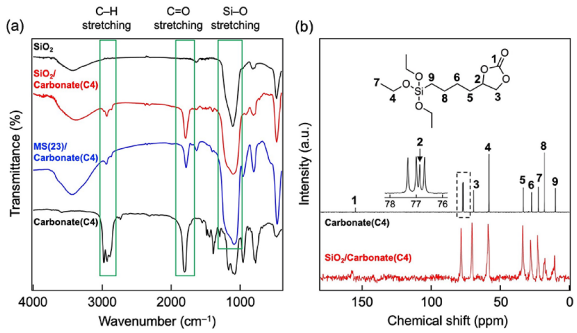


**Figure 1.** Characterization of representative catalysts. (a) IR spectra of $SiO_2$, $SiO_2$/carbonate(C4), MS(23)/carbonate(C4), and carbonate(C4). (b) $^{13}$C NMR spectra of carbonate(C4) and $SiO_2$/carbonate(C4).

carbonate groups connect with silica surface mainly through T$^2$ site (Figure S1), which indicated that approximately 4−5 equiv of residual silanol with respect to carbonate was present on the prepared catalysts.

$SiO_2$/carbonate(C*n*) and MS(23)/carbonate(C*n*) were applied to the catalytic hydrosilylation of 4-chlorobenzaldehyde (**1a**) with dimethylphenylsilane (**2a**) (Figure 2). The

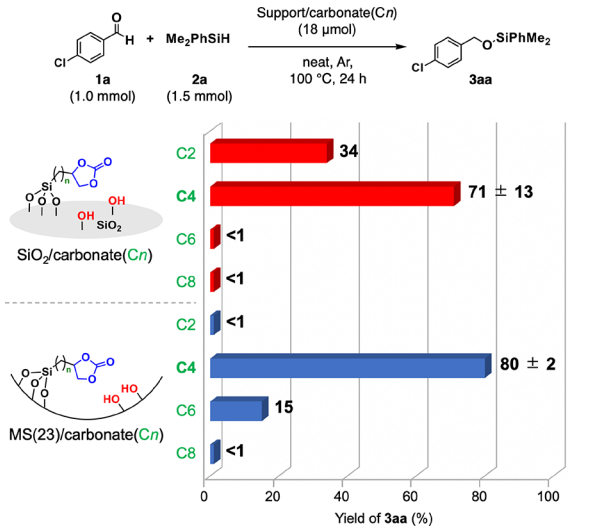


**Figure 2.** Effect of linker length of immobilized cyclic carbonates on the product yield. Standard deviations were evaluated for C4 catalysts using samples in different batches.

linker length had a critical impact on the catalytic performance, and the highest yield of silyl ether **3aa** was observed at a length of C4 for both silica supports. The superior catalytic activity of C4 over C2 was ascribed to the flexibility of the methylene linker. According to a previous study on the base catalytic activity of amines immobilized on mesoporous silica (SBA-15) with methylene linker lengths of C1−C5, the promotional effect of surface silanols on catalysis was prohibited for short linkers (C1 and C2) owing to the lower conformational diversity.[17] However, the reason for low reactivities of the C6 and C8 catalysts has not been clear so far. There is a possibility that too much conformational diversity of the long chains decreased the probability of appropriate conformations for concerted catalysis with silanol, suggested by the weaker interaction of carbonate and silanol observed in infrared spectroscopy (vide infra).

To demonstrate that the hydrosilylation catalysis of cyclic carbonates emerged as a result of immobilization on silica, control experiments were conducted (Figure 3). The hydrosilylation reaction did not proceed efficiently with free carbonates, silica supports, or physical mixtures of propylene carbonate and silica supports. These results clearly indicate that immobilization of the cyclic carbonates is essential to the catalysis of $SiO_2$/carbonate(C4) and MS(23)/carbonate(C4). The lack of catalytic activity of $SiO_2$/carbonate(C4)-capped, which was obtained by capping the surface silanols of $SiO_2$/carbonate(C4) with a methyl group, suggests that the role of the silica support is to activate the carbonyl group of **1a** using the surface Si−OH groups as the acid sites.[16−21] In addition, it was found that the ratio of silanol to carbonate was an important factor: $SiO_2$/carbonate(C4)-**2**, which was prepared with the amount of the carbonate(C4) precursor 2 times



https://doi.org/10.1021/jacsau.3c00306
JACS Au 2023, 3, 2692−2697

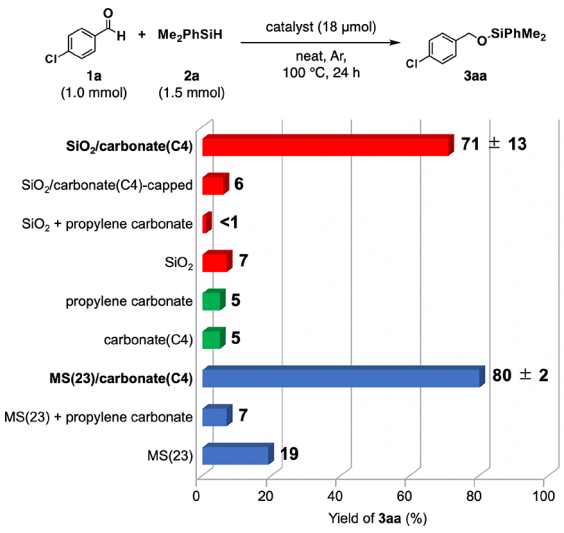


**Figure 3.** Emergence of the hydrosilylation catalysis of cyclic carbonates by immobilization on a silica support.

higher than that of $SiO_2$/carbonate(C4), afforded no reaction product. On the other hand, the reduction of carbonate loading on MS(23)/carbonate(C4) did not change the product yield: the catalysts with carbon contents of 7.8 and 5.5 mmol $g^{-1}$ showed **3aa** yields of 80% and 81%, respectively.

The proximity of the immobilized carbonate and surface silanol was evidenced by FT-IR spectroscopy. The IR spectra of $SiO_2$/carbonate(C*n*) (Figures 4a–f) revealed that only

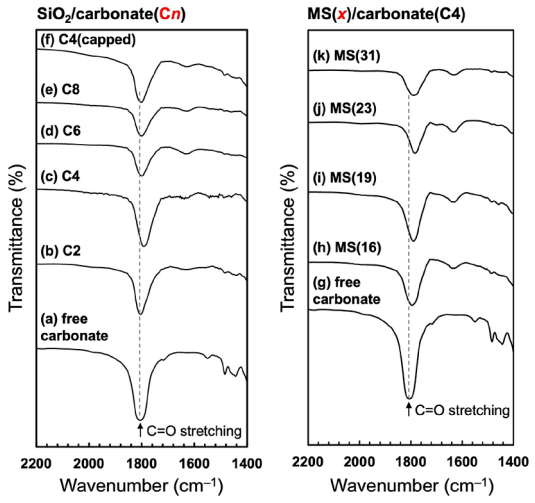


**Figure 4.** Effects of linker length (left) and pore size (right) on the C═O stretching frequency of $SiO_2$/carbonate(C*n*) and MS(*x*)/carbonate(C4), respectively. FT-IR spectra of (a, g) carbonate(C4) before immobilization, (b) $SiO_2$/carbonate(C2), (c) $SiO_2$/carbonate-(C4), (d) $SiO_2$/carbonate(C6), (e) $SiO_2$/carbonate(C8), (f) $SiO_2$/carbonate(C4)-capped, (h) MS(16)/carbonate(C4), (i) MS(19)/carbonate(C4), (j) MS(23)/carbonate(C4), and (k) MS(31)/carbonate(C4).

$SiO_2$/carbonate(C4) showed a significant negative shift in the C═O stretching frequency (Figure 4c). Considering the result for $SiO_2$/carbonate(C4)-capped (Figure 4f), this red shift was attributed to the hydrogen bonding interaction between silanol and carbonate. It was reported that the coordination of carbonyl group of cyclic carbonates to acidic site induced the decrease of C═O stretching frequency.[32] Based on the results shown in Figures 2, 3, and 4a–f, a plausible reaction mechanism is proposed, as shown in Scheme 2. The aldehyde

**Scheme 2. Proposed Reaction Mechanism**

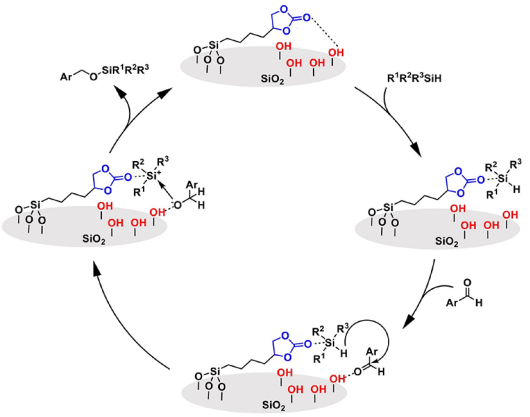


and silane are concertedly activated by a paired silanol and carbonate and undergo efficient hydride transfer, followed by silyl transfer. This mechanism contrasts the mechanism established for boron-based Lewis acid organocatalyst, in which silyl transfer occurs before hydride transfer (Scheme S2).[33−38]

Furthermore, the pore size effects of the MS support on the catalytic activity and C═O stretching frequency of the immobilized carbonate(C4) were investigated. Table 1 and

**Table 1. Pore Size Effect on Product Yield**

| entry | support of carbonate(C4) | yield of **3aa** (%)[a] |
|---|---|---|
| 1 | MS(16) | 20 |
| 2[b] | MS(19) | 18 |
| 3 | MS(23) | 80 |
| 4 | MS(31) | 37 |

[a]Determined by $^1$H NMR. [b]Dibenzyl ether was formed as a byproduct with 22% yield.

Figures 4g–k show the catalytic activity and IR absorption by C═O stretching, respectively, of MS(*x*)/carbonate(C4) with pore diameters of 16, 19, 23, and 31 Å. The highest catalytic activity was observed at a pore size of 23 Å (entry 3). IR spectroscopy revealed that the decrease in the C═O stretching frequency was the largest for MS(23)/carbonate(C4). Thus, the reason for the highest catalytic activity is that MS(23) enabled the closest proximity of carbonate and silanol. A correlation was observed between the catalytic activities and C═O stretching frequencies of MS(*x*)/carbonate(C4) (Figure 5). The general trend of increasing catalytic activity with decreasing C═O stretching frequency supports the proposed reaction mechanism (Scheme 2), in which the proximity of the acid and base sites is essential.

The validity of the proposed reaction mechanism in Scheme 2 was further examined by DFT calculations with M08-HX functional using the Gaussian 16 program.[39−41] Model reaction system **A** consisted of **1a**, **2a**, ethylene carbonate, and a cage-shaped cluster model of $SiO_2$ (Figure S2). For computational efficiency, ethylene carbonate and the $SiO_2$ cluster model were used to mimic the active sites of the catalyst (immobilized cyclic carbonate and surface silanol, respectively).[42] Figure 6a


https://doi.org/10.1021/jacsau.3c00306
JACS Au 2023, 3, 2692−2697

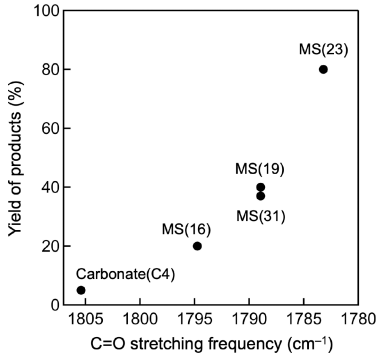


**Figure 5.** Yield of products plotted against the C═O stretching frequency of MS($x$)/carbonate(C4) and free carbonate(C4). Reaction conditions were the same as those shown in Figure 2 and Table 1. For MS(19)/carbonate(C4), the total yields of the silylation and benzylation products was plotted.

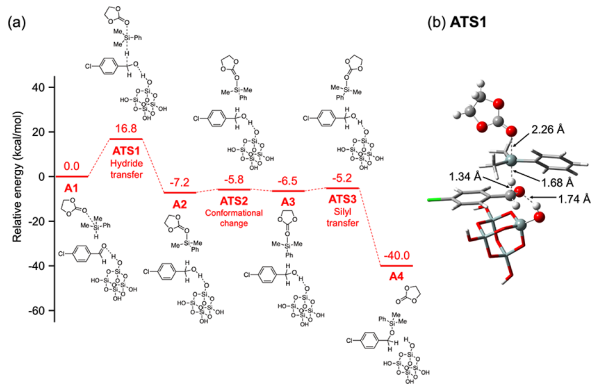


**Figure 6.** (a) Calculated energy profile for the proposed reaction mechanism (system **A**). (b) Optimized structure of **ATS1** with a length annotation. The other optimized structures are summarized in Figure S4.

shows the calculated energy profile for the proposed mechanism and schematic images of the optimized structures. The transition state of hydride transfer (**ATS1**) has an activation energy of 16.8 kcal mol$^{-1}$, whereas the subsequent conformational change and silyl transfer steps are almost barrierless. In **ATS1**, the carbonate coordinates to the Si center of the silane, whereas the silanol forms a hydrogen bond with the carbonyl oxygen of the aldehyde. Thus, the carbonate and silanol concertedly facilitate the transfer of hydride from the silane to the aldehyde. The reasonable barrier height (16.8 kcal mol$^{-1}$) suggests that the hydrosilylation reaction in a real system likely proceeds via the proposed mechanism. It was noticed that the alkoxide species generated by the hydride transfer abstracted the proton of silanol in the relaxation path from **ATS1** to **A2** and that the proton is returned to regenerate the silanol in the path from **ATS3** to **A4**, as shown in Figure S8e.

On the other hand, model systems **B** and **C**, containing only either the carbonate or silanol, respectively, have significantly larger activation energies than system **A** (Table 2 and Figure S3). Specifically, the calculated barrier heights are 25.4 and 26.8 kcal mol$^{-1}$ for **B** and **C**, respectively. In addition, the system containing only **1a** and **2a** (system **D**) has an activation energy of 33.6 kcal mol$^{-1}$. These theoretical results are consistent with the experimental observation that the hydrosilylation reaction proceeds efficiently only when immobilized carbonate catalysts are used.

**Table 2. Calculated Activation Energies ($E_a$)**

| system | catalyst | $E_a$ (kcal/mol) |
|---|---|---|
| **A** | carbonate + silanol | 16.8 |
| **B** | carbonate | 25.4 |
| **C** | silanol | 26.8 |
| **D** | none | 33.6 |

The applicability of the $SiO_2$/carbonate(C4) catalyst to the hydrosilylation reaction between other aldehydes and silanes was examined (Table 3). In addition to **1a**, benzaldehyde (**1b**), cinnamaldehyde (**1c**), and 4-(dimethylamino)benzaldehyde (**1d**) were converted into the corresponding silyl ether by using **2a** in moderate to high yields (69−94%) under the same reaction conditions. Thus, aromatic aldehydes with electron-withdrawing or electron-donating substituents can be used in this system. Among the silanes examined (**2a**−**2d**), **2c** gave the highest yield of **3ac** (83%) in the reaction with **1a**. The lower reactivity of **2b** than that of **2a** was attributed to steric hindrance. Notably, the applicability of $SiO_2$/carbonate(C4) to **1d** with a basic functional group is in sharp contrast to those of previously developed acid catalysts, such as Fe-exchanged montmorillonite (Fe-Mont) and $SiO_2$−$Al_2O_3$.[43] Using these solid acid catalysts, only trace amounts of silyl ether **3da** were obtained, owing to catalyst poisoning by the adsorption of amino groups on the acid sites. In contrast, $SiO_2$/carbonate(C4) retained its catalytic activity because of the much weaker acidity of the silanol groups.

**Table 3. Substrate Scope for Hydrosilylation Catalyzed by $SiO_2$/Carbonate(C4)**

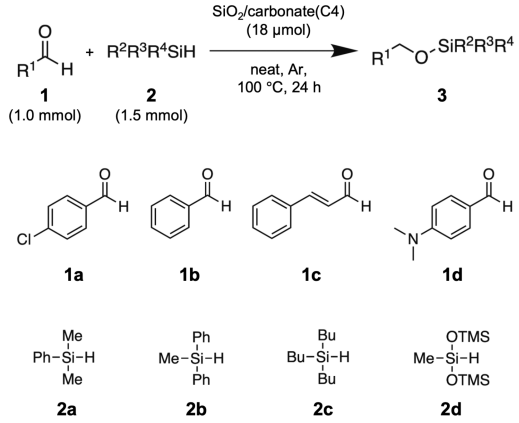


| catalyst | aldehyde | silane | yield of **3** (%)[a] |
|---|---|---|---|
| $SiO_2$/carbonate(C4) | **1a** | **2a** | 71 |
| | **1b** | **2a** | 69 |
| | **1c** | **2a** | 94 |
| | **1a** | **2b** | 44 |
| | **1a** | **2c** | 83 |
| | **1a** | **2d** | 57 |
| $SiO_2$/carbonate(C4) | **1d** | **2a** | 76 |
| Fe-Mont | **1d** | **2a** | trace |
| $SiO_2$−$Al_2O_3$ | **1d** | **2a** | trace |

[a]Determined by $^1$H NMR.

In summary, novel silica-immobilized carbonate catalysts, $SiO_2$/carbonate(C$n$) and MS($x$)/carbonate(C$n$), were systematically prepared by varying the structural parameters. Catalytic


https://doi.org/10.1021/jacsau.3c00306
JACS Au 2023, 3, 2692−2697

hydrosilylation of aldehydes emerged as a result of the synergy between the carbonates and surface silanol groups. C4-linker and MS(23) were found to be optimal for catalysis, although effects of conformational diversity of linkers, surface area, and functional group density should be investigated in future studies for more detailed understanding of the surface phenomena. The carbonate and silanol were proposed to concertedly activate the silane and aldehyde, respectively, for efficient hydride transfer. IR spectroscopy and DFT calculations supported the proposed mechanism. $SiO_2$/carbonate-(C4) could catalyze the hydrosilylation of a substrate with an amino group, owing to the mild acidity of silanol, which is a clear advantage over previously reported acid catalysts. These findings provide a stepping stone for the development of more functionalized heterogeneous organocatalysts.

## ■ ASSOCIATED CONTENT

### Supporting Information

The Supporting Information is available free of charge at https://pubs.acs.org/doi/10.1021/jacsau.3c00306.

> Detailed procedures for experiments and theoretical calculations, results of elemental analysis, calculated energy profiles and optimized structures of model reaction systems **A**–**D**, interatomic distance at each step of the reaction of model system **A**, characterization data for catalyst precursors and products of catalytic reactions, and Cartesian coordinates of the calculated structures (PDF)

## ■ AUTHOR INFORMATION


### Corresponding Author

**Ken Motokura** − *Department of Chemistry and Life Science, Yokohama National University, Yokohama 240-8501, Japan; Department of Chemical Science and Engineering, School of Materials and Chemical Technology, Tokyo Institute of Technology, Yokohama 226-8502, Japan;* orcid.org/0000-0002-0066-5139; Email: motokura-ken-xw@ynu.ac.jp

### Authors

**Shingo Hasegawa** − *Department of Chemistry and Life Science, Yokohama National University, Yokohama 240-8501, Japan;* orcid.org/0000-0001-5295-017X

**Keisuke Nakamura** − *Department of Chemical Science and Engineering, School of Materials and Chemical Technology, Tokyo Institute of Technology, Yokohama 226-8502, Japan*

**Kosuke Soga** − *Department of Chemistry and Life Science, Yokohama National University, Yokohama 240-8501, Japan*

**Kei Usui** − *Department of Chemical Science and Engineering, School of Materials and Chemical Technology, Tokyo Institute of Technology, Yokohama 226-8502, Japan*

**Yuichi Manaka** − *Department of Chemical Science and Engineering, School of Materials and Chemical Technology, Tokyo Institute of Technology, Yokohama 226-8502, Japan; Renewable Energy Research Center, National Institute of Advanced Industrial Science and Technology (AIST), Koriyama 963-0298, Japan*

Complete contact information is available at: https://pubs.acs.org/10.1021/jacsau.3c00306


### Author Contributions

CRediT: **Shingo Hasegawa** data curation, investigation, writing-original draft; **Keisuke Nakamura** data curation, formal analysis, investigation; **Kosuke Soga** data curation, formal analysis, investigation; **Kei Usui** data curation, formal analysis, investigation; **Yuichi Manaka** formal analysis, supervision; **Ken Motokura** conceptualization, funding acquisition, project administration, supervision, writing-review & editing.

### Notes

The authors declare no competing financial interest.

## ■ ACKNOWLEDGMENTS

This research was financially supported by a Grant-in-Aid for Scientific Research (B) (No. JP22H01863) and a Grant-in-Aid for Early-Career Scientists (No. JP23K13602) from the Japan Society for the Promotion of Science (JSPS). Calculations were partly performed at the Research Center for Computational Science, Okazaki, Japan (Project: 22-IMS-C237).

## ■ REFERENCES


(1) Sigman, M. S.; Jacobsen, E. N. Schiff Base Catalysts for the Asymmetric Strecker Reaction Identified and Optimized from Parallel Synthetic Libraries. *J. Am. Chem. Soc.* **1998**, *120*, 4901−4902.

(2) Ooi, T.; Kameda, M.; Maruoka, K. Molecular Design of a $C_2$-Symmetric Chiral Phase-Transfer Catalyst for Practical Asymmetric Synthesis of α-Amino Acids. *J. Am. Chem. Soc.* **1999**, *121*, 6519−6520.

(3) Ahrendt, K. A.; Borths, C. J.; MacMillan, D. W. C. New Strategies for Organic Catalysis: The First Highly Enantioselective Organocatalytic Diels-Alder Reaction. *J. Am. Chem. Soc.* **2000**, *122*, 4243−4244.

(4) List, B.; Lerner, R. A.; Barbas, C. F. Proline-Catalyzed Direct Asymmetric Aldol Reactions. *J. Am. Chem. Soc.* **2000**, *122*, 2395−2396.

(5) Jones, S. B.; Simmons, B.; Mastracchio, A.; MacMillan, D. W. C. Collective Synthesis of Natural Products by Means of Organocascade Catalysis. *Nature* **2011**, *475*, 183.

(6) Wheeler, S. E.; Seguin, T. J.; Guan, Y.; Doney, A. C. Noncovalent Interactions in Organocatalysis and the Prospect of Computational Catalyst Design. *Acc. Chem. Res.* **2016**, *49*, 1061−1069.

(7) Kondoh, A.; Ishikawa, S.; Terada, M. Development of Chiral Ureates as Chiral Strong Brønsted Base Catalysts. *J. Am. Chem. Soc.* **2020**, *142*, 3724−3728.

(8) Ishihara, H.; Huang, J.; Mochizuki, T.; Hatano, M.; Ishihara, K. Enantio- and Diastereoselective Carbonyl-Ene Cyclization-Acetalization Tandem Reaction Catalyzed by Tris(pentafluorophenyl)borane-Assisted Chiral Phosphoric Acids. *ACS Catal.* **2021**, *11*, 6121−6127.

(9) Li, Q.; Levi, S. M.; Wagen, C. C.; Wendlandt, A. E.; Jacobsen, E. N. Site-Selective, Stereocontrolled Glycosylation of Minimally Protected Sugars. *Nature* **2022**, *608*, 74−79.

(10) Tokuhiro, Y.; Yoshikawa, K.; Murayama, S.; Nanjo, T.; Takemoto, Y. Highly Stereoselective, Organocatalytic Mannich-type Addition of Glyoxylate Cyanohydrin: A Versatile Building Block for the Asymmetric Synthesis of β-Amino-α-ketoacids. *ACS Catal.* **2022**, *12*, 5292−5304.

(11) Grimm, J. A. A.; Zhou, H.; Properzi, R.; Leutzsch, M.; Bistoni, G.; Nienhaus, J.; List, B. Catalytic Asymmetric Synthesis of Cannabinoids and Menthol from Neral. *Nature* **2023**, *615*, 634−639.

(12) Formica, M.; Rogova, T.; Shi, H.; Sahara, N.; Ferko, B.; Farley, A. J. M.; Christensen, K. E.; Duarte, F.; Yamazaki, K.; Dixon, D. J. Catalytic Enantioselective Nucleophilic Desymmetrization of Phosphonate Esters. *Nat. Chem.* **2023**, *15*, 714−721.

(13) Lee, H.-J.; Maruoka, K. Recent Asymmetric Phase-Transfer Catalysis with Chiral Binaphthyl-Modified and Related Phase-Transfer Catalysts over the Last 10 Years. *Chem. Rec.* **2023**, *23*, e202200286.

(14) Kubota, Y.; Goto, K.; Miyata, S.; Goto, Y.; Fukushima, Y.; Sugi, Y. Enhanced Effect of Mesoporous Silica on Base-Catalyzed Aldol Reaction. *Chem. Lett.* **2003**, *32*, 234−235.
(15) Bass, J. D.; Anderson, S. L.; Katz, A. The Effect of Outer-Sphere Acidity on Chemical Reactivity in a Synthetic Heterogeneous Base Catalyst. *Angew. Chem., Int. Ed.* **2003**, *42*, 5219−5222.
(16) Bass, J. D.; Solovyov, A.; Pascall, A. J.; Katz, A. Acid-Base Bifunctional and Dielectric Outer-Sphere Effects in Heterogeneous Catalysis: A Comparative Investigation of Model Primary Amine Catalysts. *J. Am. Chem. Soc.* **2006**, *128*, 3737−3747.
(17) Brunelli, N. A.; Didas, S. A.; Venkatasubbaiah, K.; Jones, C. W. Tuning Cooperativity by Controlling the Linker Length of Silica-Supported Amines in Catalysis and $CO_2$ Capture. *J. Am. Chem. Soc.* **2012**, *134*, 13950−13953.
(18) Brunelli, N. A.; Venkatasubbaiah, K.; Jones, C. W. Cooperative Catalysis with Acid-Base Bifunctional Mesoporous Silica: Impact of Grafting and Co-condensation Synthesis Methods on Material Structure and Catalytic Properties. *Chem. Mater.* **2012**, *24*, 2433−2442.
(19) Brunelli, N. A.; Jones, C. W. Tuning Acid-Base Cooperativity to Create Next Generation Silica-Supported Organocatalysts. *J. Catal.* **2013**, *308*, 60−72.
(20) Kim, K. C.; Moschetta, E. G.; Jones, C. W.; Jang, S. S. Molecular Dynamics Simulations of Aldol Condensation Catalyzed by Alkylamine-Functionalized Crystalline Silica Surface. *J. Am. Chem. Soc.* **2016**, *138*, 7664−7672.
(21) Collier, V. E.; Ellebracht, N. C.; Lindy, G. I.; Moschetta, E. G.; Jones, C. W. Kinetic and Mechanistic Examination of Acid-Base Bifunctional Aminosilica Catalysts in Aldol and Nitroaldol Condensation. *ACS Catal.* **2016**, *6*, 460−468.
(22) Motokura, K.; Tada, M.; Iwasawa, Y. Heterogeneous Organic Base-Catalyzed Reactions Enhanced by Acid Supports. *J. Am. Chem. Soc.* **2007**, *129*, 9540−9541.
(23) Motokura, K.; Tada, M.; Iwasawa, Y. Cooperative Catalysis of Primary and Tertiary Amines on Oxide Support Surface for One-Pot C−C Bond Forming Reactions. *Angew. Chem., Int. Ed.* **2008**, *47*, 9230−9235.
(24) Copéret, C.; Comas-Vives, A.; Conley, M. P.; Estes, D. P.; Fedorov, A.; Mougel, V.; Nagae, H.; Núñez-Zarur, F.; Zhizhko, P. A. Surface Organometallic and Coordination Chemistry toward Single-Site Heterogeneous Catalysts: Strategies, Methods, Structures, and Activities. *Chem. Rev.* **2016**, *116*, 323−421.
(25) Copéret, C.; Allouche, F.; Chan, K. W.; Conley, M. P.; Delley, M. F.; Fedorov, A.; Moroz, I. B.; Mougel, V.; Pucino, M.; Searles, K.; Yamamoto, K.; Zhizhko, P. A. Bridging the Gap between Industrial and Well-Difined Supported Catalysts. *Angew. Chem., Int. Ed.* **2018**, *57*, 6398−6440.
(26) Motokura, K.; Ding, S.; Usui, K.; Kong, Y. Enhanced Catalysis Based on the Surface Environment of the Silica-Supported Metal Complex. *ACS Catal.* **2021**, *11*, 11985−12018.
(27) Schäffner, B.; Schäffner, F.; Verevkin, S. P.; Börner, A. Organic Carbonates as Solvents in Synthesis and Catalysis. *Chem. Rev.* **2010**, *110*, 4554−4581.
(28) Shaikh, R. R.; Pornpraprom, S.; D'Elia, V. Catalytic Strategies for the Cycloaddition of Pure, Diluted, and Waste $CO_2$ to Epoxides under Ambient Conditions. *ACS Catal.* **2018**, *8*, 419−450.
(29) Guo, L.; Lamb, K. J.; North, M. Recent Developments in Organocatalyzed Transformations of Epoxides and Carbon Dioxide into Cyclic Carbonates. *Green Chem.* **2021**, *23*, 77−118.
(30) Motokura, K.; Ikeda, M.; Nambo, M.; Chun, W.-J.; Nakajima, K.; Tanaka, S. Concerted Catalysis in Tight Spaces: Palladium-Catalyzed Allylation Reactions Accelerated by Accumulated Active Sites in Mesoporous Silica. *ChemCatChem.* **2017**, *9*, 2924−2929.
(31) Usui, K.; Manaka, Y.; Chun, W.-J.; Motokura, K. Rhodium-Iodide Complex on a Catalytically Active $SiO_2$ Surface for One-Pot Hydrosilylation-$CO_2$ Cycloaddition. *Chem.—Eur. J.* **2022**, *28*, No. e202104001.
(32) Fulfer, K. D.; Kuroda, D. G. Solvation Structure and Dynamics of the Lithium Ion in Organic Carbonate-Based Electrolytes: A Time-Dependent Infrared Spectroscopy Study. *J. Phys. Chem. C* **2016**, *120*, 24011−24022.
(33) Parks, D. J.; Piers, W. E. Tris(pentafluorophenyl)boron-Catalyzed Hydrosilylation of Aromatic Aldehydes, Ketones, and Esters. *J. Am. Chem. Soc.* **1996**, *118*, 9440−9441.
(34) Parks, D. J.; Blackwell, J. M.; Piers, W. E. Studies on the Mechanism of $B(C_6F_5)_3$-Catalyzed Hydrosilation of Carbonyl Functions. *J. Org. Chem.* **2000**, *65*, 3090−3098.
(35) Rendler, S.; Oestreich, M. Conclusive Evidence for an $S_N2$-Si Mechanism in the $B(C_6F_5)_3$-Catalyzed Hydrosilylation of Carbonyl Compounds: Implications for the Related Hydrogenation. *Angew. Chem., Int. Ed.* **2008**, *47*, 5997−6000.
(36) Hog, D. T.; Oestreich, M. B. $C_6F_5)_3$-Catalyzed Reduction of Ketones and Imines Using Silicon-Stereogenic Silanes: Stereoinduction by Single-Poing Binding. *Eur. J. Org. Chem.* **2009**, *2009*, 5047−5056.
(37) Sakata, K.; Fujimoto, H. Quantum Chemical Study of $B(C_6F_5)_3$-Catalyzed Hydrosilylation of Carbonyl Group. *J. Org. Chem.* **2013**, *78*, 12505−12512.
(38) Denmark, S. E.; Ueki, Y. Lewis Base Activation of Lewis Acids: Group 13. In Situ Generation and Reaction of Borenium Ions. *Organometallics* **2013**, *32*, 6631−6634.
(39) Frisch, M. J.; Trucks, G. W.; Schlegel, H. B.; Scuseria, G. E.; Robb, M. A.; Cheeseman, J. R.; Scalmani, G.; Barone, V.; Petersson, G. A.; Nakatsuji, H.; Li, X.; Caricato, M.; Marenich, A. V.; Bloino, J.; Janesko, B. G.; Gomperts, R.; Mennucci, B.; Hratchian, H. P.; Ortiz, J. V.; Izmaylov, A. F.; Sonnenberg, J. L.; Williams-Young, D.; Ding, F.; Lipparini, F.; Egidi, F.; Goings, J.; Peng, B.; Petrone, A.; Henderson, T.; Ranasinghe, D.; Zakrzewski, V. G.; Gao, J.; Rega, N.; Zheng, G.; Liang, W.; Hada, M.; Ehara, M.; Toyota, K.; Fukuda, R.; Hasegawa, J.; Ishida, M.; Nakajima, T.; Honda, Y.; Kitao, O.; Nakai, H.; Vreven, T.; Throssell, K.; Montgomery, J. A., Jr.; Peralta, J. E.; Ogliaro, F.; Bearpark, M. J.; Heyd, J. J.; Brothers, E. N.; Kudin, K. N.; Staroverov, V. N.; Keith, T. A.; Kobayashi, R.; Normand, J.; Raghavachari, K.; Rendell, A. P.; Burant, J. C.; Iyengar, S. S.; Tomasi, J.; Cossi, M.; Millam, J. M.; Klene, M.; Adamo, C.; Cammi, R.; Ochterski, J. W.; Martin, R. L.; Morokuma, K.; Farkas, O.; Foresman, J. B.; Fox, D. J. *Gaussian 16*; Gaussian, Inc., Wallingford CT, 2016.
(40) Zhao, Y.; Truhlar, D. G. Exploring the Limit of Accuracy of the Global Hybrid Meta Density Functional for Main-Group Thermochemistry, Kinetics, and Noncovalent Interactions. *J. Chem. Theory Comput.* **2008**, *4*, 1849−1868.
(41) Mardirossian, N.; Head-Gordon, M. How Accurate Are the Minnesota Density Functionals for Noncovalent Interactions, Isomerization Energies, Thermochemistry, and Barrier Heights Involving Molecules Composed of Main-Group Elements? *J. Chem. Theory Comput.* **2016**, *12*, 4303−4325.
(42) Rimola, A.; Costa, D.; Sodupe, M.; Lambert, J.-F.; Ugliengo, P. Silica Surface Features and Their Role in the Adsorption of Biomolecules: Computational Modeling and Experiments. *Chem. Rev.* **2013**, *113*, 4216−4313.
(43) Onaka, M.; Higuchi, K.; Nanami, H.; Izumi, Y. Reduction of Carbonyl Compounds with Hydrosilanes on Solid Acid and Solid Base. *Bull. Chem. Soc. Jpn.* **1993**, *66*, 2638−2645.


https://doi.org/10.1021/jacsau.3c00306
*JACS Au* 2023, 3, 2692−2697